water

MDPI

Article

Spatial-Temporal Variations of Drought-Flood Abrupt Alternation Events in Southeast China

Bowen Zhang [1], Ying Chen [1,2,*], Xingwei Chen [1,2], Lu Gao [1,2] and Meibing Liu [1,2]

[1] School of Geographical Sciences, Fujian Normal University, Fuzhou 350007, China; 17693219112@163.com (B.Z.)
[2] State Key Laboratory for Subtropical Mountain Ecology of the Ministry of Science and Technology and Fujian Province, Fujian Normal University, Fuzhou 350007, China
* Correspondence: chenying_nju@163.com

Abstract: Under climate change, the frequency of drought-flood abrupt alternation (DFAA) events is increasing in Southeast China. However, there is limited research on the evolution characteristics of DFAA in this region. This study evaluated the effectiveness of the drought and flood indexes including SPI (Standardized Precipitation Index), SPEI (Standardized Precipitation Evapotranspiration Index), and SWAP (Standardized Weighted Average Precipitation Index) in identifying DFAA events under varying days of antecedent precipitation. Additionally, the evolution characteristics of DFAA events in Fujian Province from 1961 to 2021 were explored. The results indicate that (1) SPI-12d had the advantages of high effectiveness, optimal generalization accuracy, and strong generalization ability of identification results, and it can be used as the optimal identification index of DFAA events in Southeast China. (2) There was an overall increase in DFAA events at a rate of 1.8 events/10a. The frequency of DFAA events showed a gradual increase from the northwest to the southeast. (3) DTF events were characterized by moderate drought to flood, particularly in February, July, and August, while FTD events were characterized by light/moderate flood to drought, with more events occurring from June to October. (4) DTF event intensity increased in the northern and western regions from 1961 to 2021. For FTD events, the intensity notably increased in the western region from 1961 to 2001, while a significant increase occurred in all regions except the central region from 2001 to 2021. These findings emphasize the need for precautionary measures to address the increasing frequency and severity of DFAA events in Southeast China.

Keywords: drought-flood abrupt alternation; identification index; temporal and spatial evolution; Fujian province

Citation: Zhang, B.; Chen, Y.; Chen, X.; Gao, L.; Liu, M. Spatial-Temporal Variations of Drought-Flood Abrupt Alternation Events in Southeast China. *Water* **2024**, *16*, 498. https://doi.org/10.3390/w16030498

Academic Editor: Songhao Shang

Received: 19 December 2023
Revised: 26 January 2024
Accepted: 1 February 2024
Published: 4 February 2024

1. Introduction

Drought-flood abrupt alternation (DFAA) is a natural phenomenon characterized by the rapid alternation of droughts and floods over a short period, encompassing both drought-to-flood (DTF) and flood-to-drought (FTD) variations. Given the concurrent presence of droughts and floods and the swiftness of their transitions, DFAA events tend to pose a greater level of hazard compared to isolated droughts or floods. In the context of global warming [1,2], intensified extreme precipitation, and enhanced water–air interactions, the climate system has exhibited reduced stability [1,3–5]. The uneven spatial and temporal distribution of precipitation is further exacerbated by the combined effects of climate change and human activities [6], leading to an increased likelihood and frequency of DFAA [7–9].

Based on the current understanding, the identification of DFAA can be broadly categorized into two main approaches. The first method is to directly construct the DFAA indexes. These indexes primarily include the Long-cycle Drought-Flood Abrupt Alternation Index (LDFAI) [10], the Short-cycle Drought-Flood Abrupt Alternation Index (SDFAI) [11,12], and the daily-scale Drought and Flood Rapid Transition Index (DWAAI) [13]. Among these

indexes, the LDFAI and SDFAI predominantly identify drought-flood abrupt transition events on a monthly or even seasonal scale. The LDFAI generally focuses on selecting DFAA events occurring between April and September, and the SDFAI narrows down the time scale from neighboring seasons to neighboring months by keeping the basic structure of the LDFAI. The identification based on the monthly or even seasonal scale has often led to the neutralization of drought and flood signals, resulting in less accurate identification of DFAA. Additionally, the LDFAI and SDFAI fail to fully capture the timing of emergent events and the multidimensional characteristics of DFAA [14–16]. The DWAAI, which identifies DFAA events on a daily time scale, can assess the difference in intensity between droughts and floods during early and late stages as well as determine the urgency of transitioning. However, the parameter involved in the DWAAI (i.e., the attenuation coefficient) needs to be adjusted according to the geographical environment [17,18]. Additionally, the range of drought and flood values varies across different regions, which lacks consistency.

The second method is based on the combination of drought and flood indexes, such as the Standardized Precipitation Index (SPI) [8,19], the Standardized Precipitation Evapotranspiration Index (SPEI) [7,20–22], the Standardized Weighted Average Precipitation Index (SWAP) [23], and the concept of travel theory to identify DFAA. It allows for the analysis of DFAA on a daily time scale. However, it is worth noting that there may be different DFAA events based on different drought and flood indexes. Their suitability should be evaluated based on the specific characteristics of the study area. The SPEI has better applicability than the SPI in assessing drought and flood in Northeast China [24]. Similar results can be found in [25]. Yang et al. [26] revealed that the SWAP index, combined with the multi-threshold run theory enables a more accurate identification of DFAA events in the Yangtze River basin [27–29]. The study found that the SPI and SPEI have strong monitoring ability for drought in the southern part of northern China. Liang et al. [30] found that the SWAP index is highly applicable in identifying short-period drought-flood abrupt change events in the Pearl River Basin by comparing the SPI, SPEI, and SWAP. However, the suitability evaluation of drought and flood indexes in DFAA identification is limited. The suitability evaluation of the drought and flood indicators is a prerequisite for the use of the second method to study DFAA.

In recent years, there has been a gradual increase in the frequency of DFAA in China [7,31,32]. Studies on DFAA in China are mainly focused on the Yangtze River Basin, Huaihe River Basin, Pearl River Basin, and Southwest China [12,33–35]. Like other regions in China, the southeastern coastal region has also been experiencing more frequent and intense droughts and floods, making the issue of DFAA a significant problem [15,32,36].

We aimed to evaluate the spatial-temporal evolution patterns of DFAA in Southeast China from 1961 to 2021. Specifically, using Fujian Province as a case study, the objectives of this study were to (1) evaluate different DFFA indexes involving SPI, SPEI, and SWAP under varying days of antecedent precipitation for the study area; (2) explore the spatial-temporal evolution characteristic of DFAA in Fujian Province over the past 60 years. The results of this study will provide a scientific foundation for identifying, diagnosing, predicting, and warning about regional drought and flood hazards as well as assessing risks.

2. Data and Methods

2.1. Study Area and Data

Fujian Province is located at 23°33′~28°20′ N and 115°50′ and 120°40′ E, with a land area of 121,400 km^2. The climate is characterized as a subtropical oceanic monsoon with an average annual temperature and precipitation ranging from approximately 17 to 21 °C and 1400 to 2000 mm, respectively. More than 80% of the total area is occupied by mountainous and hilly terrain, with a highest elevation of 2200 m and an average elevation of 300 m.

Drought and flood disasters are one of the major natural disasters in Fujian Province. In recent years, under the influence of global warming, the frequency of drought and flood disasters in the study area has increased, and the transition between drought and flood has become more frequent in a relatively short time period. Recent DFAA events occurred in

the study area, such as the 2018-09 drought to flood transition experiences in the coastal area. The continuous spring and summer drought in 2018 was the most meteorological drought in the past 15 years. The southern coastal areas and inland areas were severely affected until the middle of August. Then the study area was continuously affected by the low-pressure system, and heavy rainstorms occurred in coastal areas. Finally, the heavy rainstorms ended the long drought (from March to August 2023), and a rapid drought-to-flood transition event occurred in the coastal area, which resulted in the economic and environmental impacts from the extremes.

Daily meteorological data (precipitation, relative humidity, atmospheric pressure, minimum and maximum temperatures, wind speed, and sunshine hours) between 1961 and 2021 was obtained from the National Meteorological Information Center (NMIC) of China as well as the altitude and latitude of each station. The data were recorded from 63 meteorological stations (Figure 1) in Fujian Province. The original data underwent a rigorous process of organization, validation, and quality assurance.

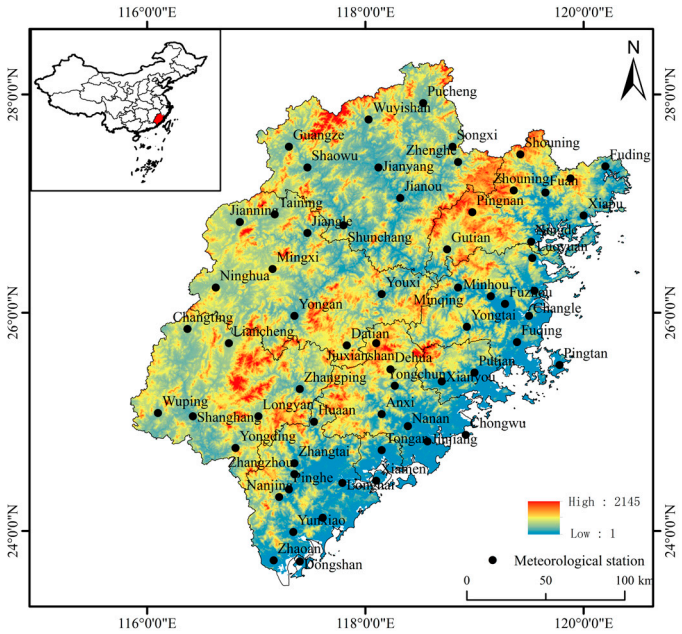

Figure 1. The location of the study area and the distribution of meteorological stations in Fujian Province.

2.2. Methods

2.2.1. Drought and Flood Indexes

In this paper, the SPI, SPEI, and SWAP were used for the determination of DFAA. The difference lies in the different focuses of construction, where the SPI only focuses on precipitation, the SPEI adds the influence of evapotranspiration, and the SWAP considers the factor of precipitation-affecting attenuation.

The SPI is an index representing the probability of rainfall occurrence in a certain period of time in a region. It has the advantages of simple calculation and stability, and it eliminates the temporal and spatial difference of rainfall. McKee [37] proposed the SPI in 1993 and used it to assess climate and drought change. A more detailed information can be found in [25].

The SPEI was proposed by [25] based on the SPI, and it incorporates the effects of temperature and precipitation on drought. It also considers evapotranspiration comprehensively through the introduction of potential evapotranspiration (PET), which combines the sensitivity of the PDSI to evapotranspiration and the multiscale characteristics of the SPI [38]. The computational process is described in detail in the literature, where the potential evapotranspiration (PET) is calculated using the FAO Penman–Monteith formula recommended by the Food and Agriculture Organization (FAO) of the United Nations.

The SWAP, proposed by Lu [39], provides a comprehensive assessment of daily drought and flood conditions across multiple timescales, including daily, weekly, monthly, and longer durations. It is a weighted average of precipitation (WAP) that considers the current precipitation, cumulative contributions, and decay effects of antecedent precipitation. While the WAP characterizes relative drought and flood conditions at a specific location, Lu et al. [40] introduced the non-dimensional SWAP index to compare drought or flood severities across different areas. The SWAP is derived from the WAP through a standardization process, transforming the gamma distribution of the WAP into a standard normal distribution.

Considering that the SPI, SPEI, and SWAP follow a consistent standardization method, their values should have the same statistical significance. Therefore, a uniform classification of flood and drought conditions standardized by a cumulative frequency distribution is used to classify drought and flooding (Table 1).

Table 1. The classification of flood and drought grades by the SPI, SPEI, and SWAP.

Grade	Type	Index Value
4	Extreme flood	≥ 2.0
3	Severe flood	$1.5 \leq$ index < 2.0
2	Moderate flood	$1.0 \leq$ index < 1.5
1	Slight flood	$0.5 \leq$ index < 1.0
0	Near normal	$-0.5 <$ index < 0.5
−1	Slight drought	$-1.0 <$ index ≤ -0.5
−2	Moderate drought	$-1.5 <$ index ≤ -1.0
−3	Severe drought	$-2.0 <$ index ≤ -1.5
−4	Extreme drought	≤ -2.0

2.2.2. Identification of DFAA Events

In this study, the daily-scale SPI, SPEI, and SWAP values were initially computed based on the daily meteorological data at each meteorological station. Subsequently, drought and flood conditions were determined based on the dryness/wetness grade classification (Table 1). Finally, these daily drought and flood conditions were integrated with the theory of run [41] to quantitatively identify drought and flood events. Referring to the related studies [42–44], the following criteria were used to identify the DFAA events.

(1) The start and end of flood and drought events: Taking flood events as an example, the interception level of the flood occurrence is 0.5 (the lower limit of a slight flood). When the SPI (SPEI or SWAP) value is larger than 0.5 for 10 consecutive days, from a special day, it is defined as a flood event. When the SPI value is less than 0.5 for 7 consecutive days, it is defined as the end of this flood event. The flood duration is the period of time between the start date and the end date of the drought event. Similarly, the beginning and ending interception levels of drought events are −0.5. The drought event is similar to the flood event and is not to be described again.

(2) The process for identifying DFAA events:

① If there successively occurs a drought event and a flood event, and the interval between the end of the drought and the start of the flood is less than 8 days, it is defined as a DFAA event. Taking a DFAA event in Fuzhou station as an example, Figure 2 shows a DTF event. The interval between drought and flood is 3 days.

② The beginning and ending times of the DFAA event coincide with those of the overall event. In Figure 2, the beginning time is the 9th and the ending time is the 58th.

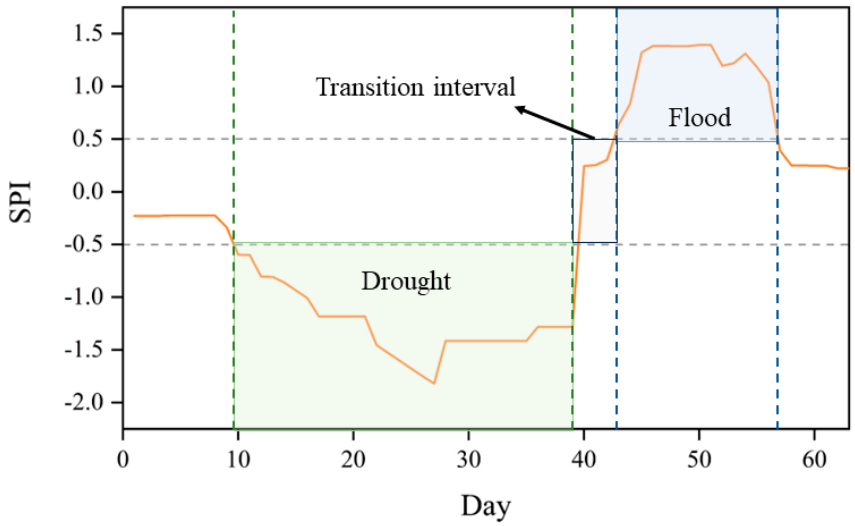

Figure 2. The identification diagram of drought-to-flood events.

③ When the DFAA event is identified, it is necessary to further determine the intensity of the event. The intensity of the DFAA is calculated according to Equation (1).

$$K = \frac{\left|\sum^{D} \text{index}_{after} - \sum^{D} \text{index}_{before}\right|}{D} \quad (1)$$

where $\sum^{D} \text{index}_{after}$ is the cumulative value of the index after the sharp turning point, $\sum^{D} \text{index}_{before}$ is the cumulative value of the index before the sharp turning point, and D is the time interval between the occurrence and the end of drought-flood abrupt alternation events (the sharp turning point is a special day when the drought turns into a flood). Referring to [23], Table 2 provides a classification of the intensity of DFAA events.

Table 2. The classification of DFAA intensity.

DFAA Intensity	K
Slight	$1.0 \leq K < 2.0$
Moderate	$2.0 \leq K < 3.0$
Severe	$3.0 \leq K$

2.2.3. Optimization of DFAA Indexes

Precipitation has a continuous impact on subsequent dry and wet conditions, which can be reflected by the days of antecedent precipitation [45,46]. To avoid alternating between short-term drought and flood events, the appropriate days of antecedent precipitation were selected as the impact factor for constructing the DFAA index. Therefore, the DFAA index was determined through the optimization of the number of days for antecedent precipitation and the drought and flood indexes. The DFAA indexes were determined through the optimization of the number of days for antecedent precipitation and the drought and flood indexes.

A comprehensive index weight distribution method [30,47,48] was used to determine the most appropriate index for identifying DFAA. Among the identification indexes (i.e., SPI, SPEI, and SWAP), we calculated the number of DFAA events for the same type (DTF or FTD) identified by each index for every month and then assigned a weight to each month. Based on the frequency of occurrence m ($0 \leq m \leq n$) (Figure 3). Finally, the total weight E serves as the measure of the identification index, and it is calculated as follows in Equation (2):

$$E = \sum_{t=1}^{t=T} m_i \cdot (col_i)_t \quad (2)$$

where E represents the weighted sum of DFAA events of the same type. T is the total number of months in the time series.$(col_i)_t$ denotes the logical value that indicates whether the method detects DFAA events in month t or not. Generally, a larger E indicates that the identification index has a greater ability to generalize results from other identification methods.

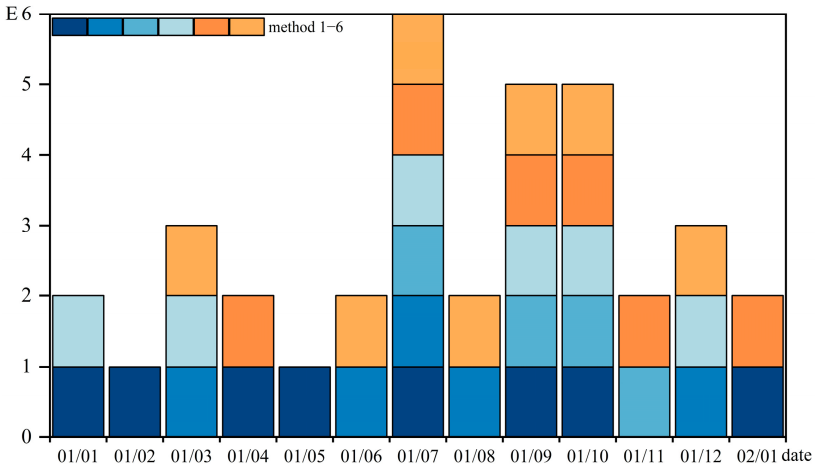

Figure 3. A schematic diagram of the weighting assignment at the monthly scale.

To avoid the scenario where an identification method with the highest number of DFAA events and low overlap with the other methods is regarded as the optimal choice, we compute E_k for the weight threshold, denoted as k ($1 \leq k \leq n$). E_k only includes the weights of the months for which $m \geq k$ and is the ratio of to the total weight (the sum of the weights when k = 1). A higher E_k indicates that there is a greater portion of DFAA events that can be jointly identified by multiple identification methods. This also suggests that the identification results are more accurate.

3. Results

3.1. Optimization of Number Days for Antecedent Precipitation

The standardized precipitation under different accumulation precipitation days shown in Figure 4. It found that the variability of standardized precipitation under the influence of antecedent rainfall was significantly flatter than when it was not influenced by antecedent rainfall (N = 1). Moreover, when the interval between two successive precipitation events is short, the standardized precipitation under the influence of antecedent precipitation consistently maintains a high value. This indicates it is more favorable for accurately reflecting the characteristics of persistent wet conditions and identifying specific flood events in the study area, considering the impacts of antecedent precipitation.

Different numbers of DFAA events were identified by the SPI, SWAP, and SPEI under the influence of different days of antecedent precipitation (Figure 5). The number of recognized DFAA events was relatively stable when the days of antecedent precipitation were 10–15 days. Therefore, we select the appropriate days of antecedent precipitation from 10 to 15 days.

The impacts of N values on the DFAA identification were assessed by the precipitation concentration index (CI) and precipitation coefficient of variation (CV); the results are shown in Table 3. It found that the minimum value of the CI is 0.48, and the maximum value of the CV is 11.86%, respectively, indicating that the precipitation events are relatively concentrated, the variability of precipitation is relatively small, and there is a high level of effectiveness in the DFAA identification for N values from 10 to 15. For N = 12, a larger CI and a smaller CV can be found for the SPI, SPEI, and SWAP. Additionally, larger weights E1 to E6 indicate a superior ability to generalize the identification results found for N = 12, which suggests that the identification results for N = 12 encompass the highest number of DFAA events that align with the identification results for the other N values. In summary,

there is a higher level of effectiveness and superior generalization ability to identify results for the SPI, SPEI, and SWAP for N = 12.

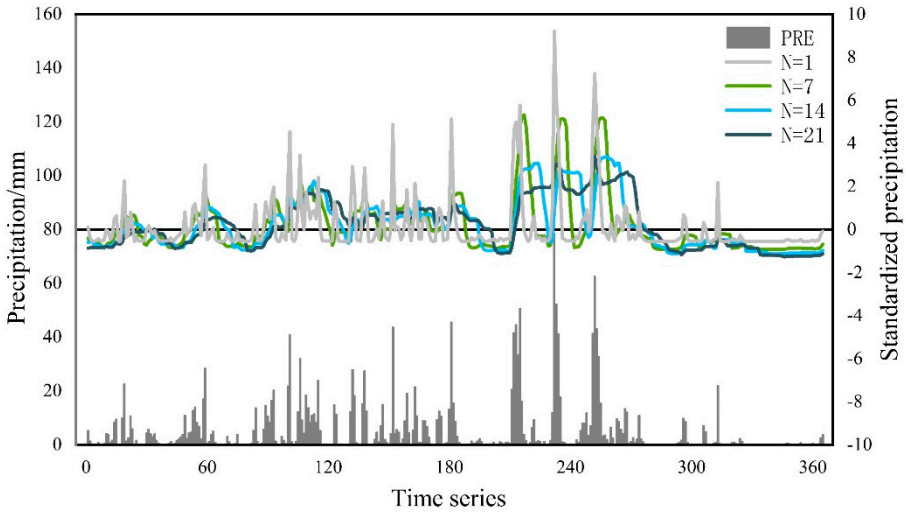

Figure 4. The standardized precipitation under different accumulation precipitation days.

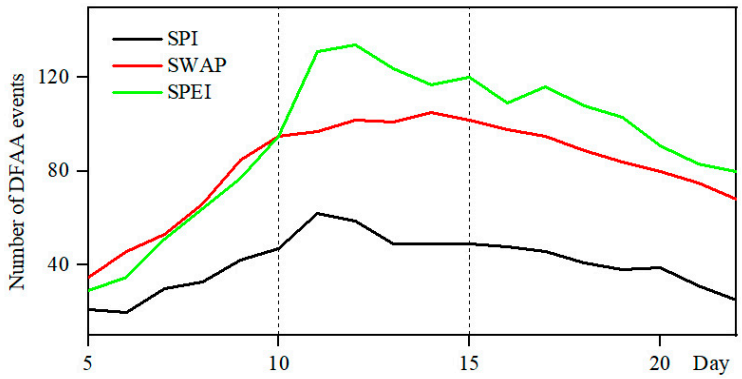

Figure 5. The number of DFAA events under the influence of different prior precipitation-affected days.

Table 3. The average assessments for different indices based on varying accumulation precipitation days.

Index	Number of Events	CI	CV	K = 1	K = 2	K = 3	K = 4	K = 5	K = 6
SPI-10	47	0.49	13.40	202	196	182	170	158	138
SPI-11	62	0.51	13.61	265	262	236	221	193	138
SPI-12	59	0.52	13.12	265	263	247	229	193	138
SPI-13	49	0.49	12.50	242	241	235	229	193	138
SPI-14	49	0.51	12.29	239	239	225	222	198	138
SPI-15	49	0.50	11.86	232	229	217	217	193	138
SWAP-10	95	0.49	12.65	467	460	452	422	394	360
SWAP-11	97	0.49	12.07	493	489	481	454	430	360
SWAP-12	102	0.49	12.37	523	521	517	487	435	360
SWAP-13	101	0.49	12.21	518	520	520	485	429	360
SWAP-14	105	0.48	12.14	516	515	495	456	424	360
SWAP-15	102	0.48	12.14	489	485	461	431	399	360
SWAP-10	95	0.49	12.65	467	460	452	422	394	360

Table 3. *Cont.*

Index	Number of Events	CI	CV	K = 1	K = 2	K = 3	K = 4	K = 5	K = 6
SPEI-10	95	0.49	13.76	463	452	450	420	404	354
SPEI-11	131	0.51	13.89	633	626	612	570	554	354
SPEI-12	134	0.51	13.39	649	645	629	581	549	354
SPEI-13	124	0.51	13.62	617	614	604	571	539	354
SPEI-14	117	0.52	13.54	606	606	594	570	554	354
SPEI-15	120	0.52	12.86	600	595	581	560	544	354
SPEI-10	95	0.49	13.76	463	452	450	420	404	354

3.2. Optimization of the SPI, SPEI, and SWAP

The statistics of the weights and the corresponding weight ratios under the three thresholds of k = 1, k = 2, and k = 3 were summarized in Table 3. It can be found that the identification accuracy is the highest for the SPI, as shown in Table 4. At k = 2, the weight ratio for the SPI is 0.8, which is higher than that of the SWAP and SPEI. This indicates that the identification results based on the SPI encompass the largest portion of events that can be jointly identified by multiple identification indexes, resulting in optimal identification accuracy of the SPI. Furthermore, when k = 3, the weight ratio for the SPI is 0.54, which is 1.6 times higher than that of the SWAP and 1.9 times higher than that for the SPEI. In summary, the SPI with 12 days of antecedent precipitation (SPI-12d) is adopted for DFAA identification in the study area.

Table 4. The detection of abrupt alternation events based on different indices under N = 12.

Index	Number of Events	CI	CV	K = 1	K = 2	K = 3
SPI-12	59	0.52	13.12	116	93	63
SWAP-12	102	0.49	12.37	180	133	63
SPEI-12	134	0.51	13.39	219	148	63

3.3. Robustness of the SPI-12d Index

To evaluate the screening capability of SPI-12d for drought identification, this study analyzed the data from the Fuzhou meteorological station as an illustrative case. As shown in Table 5, the top 10 drought events with the largest magnitudes were obtained and compared with historical disaster records at the Fuzhou station from 1961 to 2021. By comparing these drought events with the drought events documented in the disaster records for the same period, it can be observed that the drought events identified using the SPI-12d method roughly align well with the drought events recorded in the disaster records for the same time period. For instance, in 1961, a significant drought occurred in the south-central coastal area from 5 June to 30 June during the summer, and the drought events identified for the same period were from 16 June to 1 July of that year. Similarly, in 1986, there was a summer drought from 13 July to 4 August, and the selected drought events for the same period extended from 24 July to 5 August of that year. These findings are roughly consistent with the historical records as described in the literature.

It is important to note that the drought events mentioned in the literature have approximate dates, while the drought events identified based on SPI-12d may not precisely match the documented information. For example, the historical record of late September to early November in 1999 describes a prolonged period with almost 40 days of no precipitation in most of the province, characterized by continuous drought in summer and autumn. The drought events identified based on SPI-12 occurred from 7 October to 8 November, which aligns with part of the historically documented drought period. Although the onset of the drought was slightly delayed by about two weeks compared to the recorded period, it can still be considered a reasonable match. From this analysis, it becomes evident that

the SPI-12d index, when combined with the multi-threshold tour theory, is effective in identifying drought events based on SPI-12d and the theory of run.

Table 5. The identification of typical drought events based on SPI-12d and the corresponding historical records at Fuzhou station from 1960 to 2015.

No.	Start Date	End Date	Intensity	Historical Records	Source
1	3 September 2009	9 November 2009	−2.3	Continuous drought in autumn and winter	B
2	20 November 2008	4 December 2008	−2.2	Continuous drought in autumn and winter	B
3	23 September 2006	19 November 2006	−2.2	Continuous drought in summer, autumn, and winter	B
4	16 June 1961	1 July 1961	−2.2	Major drought from June 5 to June 30 in south-central Fujian coastal areas	A
5	24 July 1986	5 August 1986	−2.2	Drought in early summer from July 13 to August 4	A
6	15 September 2007	30 October 2007	−2.2	Drought occurred in early September and intensified into autumn and winter	B
7	5 October 2012	29 October 2012	−2.1	Drought occurred in mid-September, and it intensified during October along the southern coast of Fujian	B
8	26 October 2017	6 November 2017	−2.1	Drought began in late August and peaked on November 4	B
9	14 May 2000	28 May 2000	−2.1	Drought began to emerge along the coast and spread from south to north in late May	B
10	7 October 1979	8 November 1979	−2.0	Drought occurred from late September to early November	A

Note: The start date, the end date, and the intensity were identified by using SPI-12d. Sources of historical records were from (A) China Meteorological Disaster Dictionary: Fujian Volume [49] and (B) Climate Bulletin of Fujian Province (2000–2022) [50].

To validate the screening capability of SPI-12d for heavy rainfall events, the top 10 corresponding heavy rainfall events with the largest daily precipitation observations from 1961 to 2021 at Fuzhou station were selected. Table 6 displays the 10 typical rainstorm days along with the start and end dates of flood events identified by SPI-12d during the same period. Out of the 10 typical storm events, five coincided with the start date of the flood events, while the remaining five storm days fell within the flood event interval identified by SPI-12d. It can be concluded that SPI-12d is capable of capturing changes in precipitation and accurately depicting the progression of flood events.

Table 6. Rainstorm flood events corresponding to the top ten daily precipitations at the Fuzhou station.

No	Max Daily Precipitation Date	Max Daily Precipitation (mm)	Flood Start	Flood End
1	8 August 2015	244.4	8 August 2015	25 August 2015
2	28 September 2016	241.2	28 September 2016	19 October 2016
3	3 October 2005	195.6	2 October 2005	14 October 2005
4	16 July 2006	187.5	14 July 2006	6 August 2006
5	6 September 1991	170.9	6 September 1991	19 September 1991
6	5 June 1972	167.6	4 June 1972	28 June 1972
7	25 June 1991	165.4	21 June 1991	6 July 1991
8	31 August 1992	164.5	17 August 1992	16 September 1992
9	1 August 1990	163.4	1 August 1990	6 October 1990
10	4 September 1966	159.6	4 September 1966	15 September 1966

3.4. Spatial-Temporal Evolution Characteristics and Variation Diagnosis of DFAA Events

3.4.1. Temporal Evolution Characteristics and Variation Diagnosis of DFAA Events

As shown in Figure 6, there is significant variability in the number of DFAA events across 63 stations in Fujian Province from 1961 to 2021. The average number of DTF events was 39 events/a, which was significantly lower than the mean number of 50 events/a for FTD events. The DTF event number sequence generally showed a slight downward trend of 1.0/10a, while the FTD event number sequence generally showed a slight upward trend of 2.0/10a. Additionally, the DFAA event number sequence showed an upward trend of 1.8/10a.

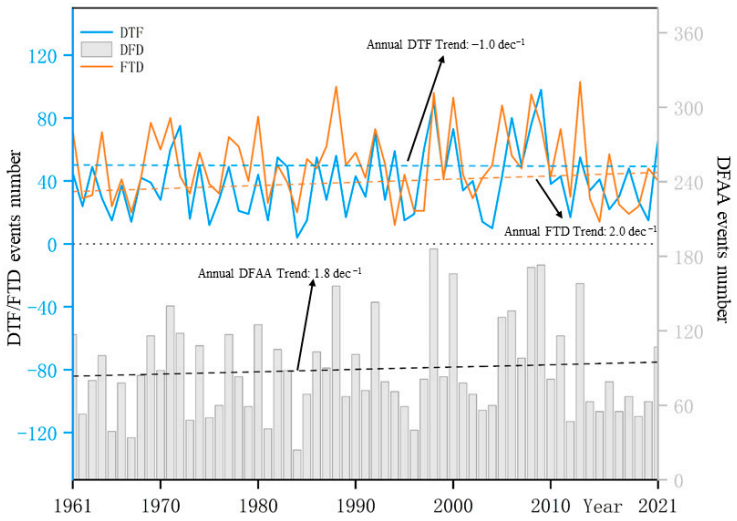

Figure 6. The number of DFAA events at 63 meteorological stations from 1961 to 2021.

The percentage of DFAA events by type in Fujian Province is shown in Figure 7. FTD events were primarily characterized by transitions from light and moderate flood to drought, with the highest percentage being light flood to medium drought events (15.79%). This was followed by moderate flood to moderate drought, light flood to severe drought, and moderate flood to light drought, with percentages of 12.59%, 11.87%, and 10.48%, respectively. As for DTF events, four types, including moderate drought to light flood, severe drought to light flood, light drought to light flood, and moderate drought to moderate floor, had a notably higher percentage. They accounted for 24.61%, 18.74%, 15.49%, and 12.37% of the total DFA events, respectively. The percentage of events between

extreme flood and extreme drought was 0.19%. However, it still deserved our attention due to its significant influence on society, ecology, agriculture, and the economy.

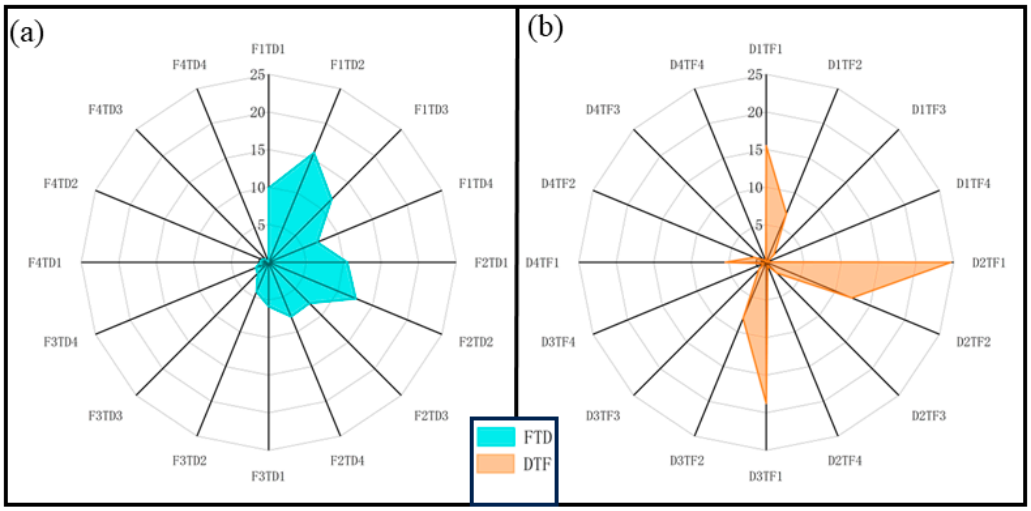

Figure 7. The percentage of (**a**) FTD events and (**b**) DTF events in Fujian Province. The values 1, 2, 3, and 4 represent light, moderate, severe, and extreme floods or droughts.

As shown in Figure 8, DTF events in the study area were distributed across the year. There were relatively lower occurrences from April to June, with frequencies of 3.54%, 3.0%, and 1.37%. In contrast, there were relatively more occurrences in February, July, and August, with frequency of 13.37%, 12.37%, and 12.74%, respectively. Additionally, light, moderate, and severe DTF events accounted for 27.70%, 62.18%, and 10.12%, respectively. In terms of DFD events, the percentages of light, moderate, and severe events were 19.58%, 64.57%, and 15.85%, respectively. The majority of these events occurred in July, September, and October, with October having the highest frequency at 29.68%. Moreover, 37.42% of the severe FTD events occurred in October.

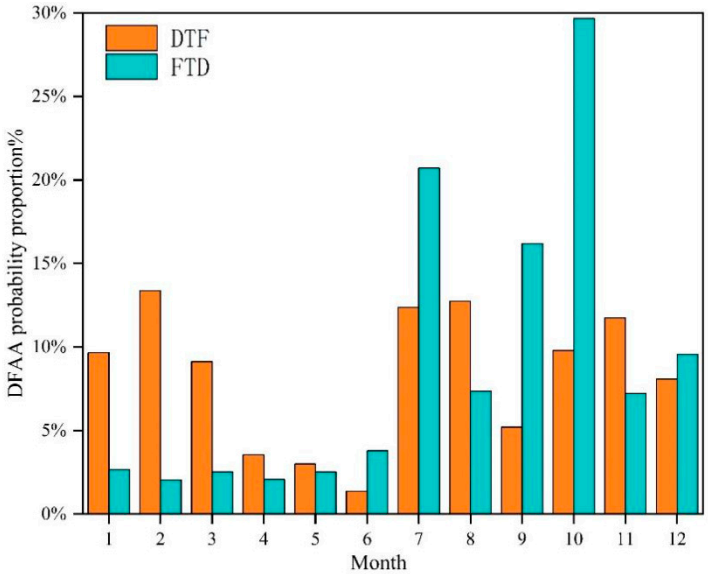

Figure 8. The intra-annual monthly frequency distribution of DFAA events in Fujian Province from 1961 to 2021.

In Figure 9a, the FTD events in January to May and in November and December are primarily characterized by light flood to drought, while the FTD events in June to October are predominantly characterized by light and moderate flood to drought. Severe

and extreme flood-to-drought events mainly occurred from July to November. In Figure 9b, DTF events are primarily characterized by transitions from moderate drought to flood. There was a notable presence of extreme drought-to-flood events in October to December and January. During these months, extreme drought to light and moderate flood events dominates. However, the frequency in February was the highest, and the transitions were mainly characterized by moderate and severe drought to light flood (61%).

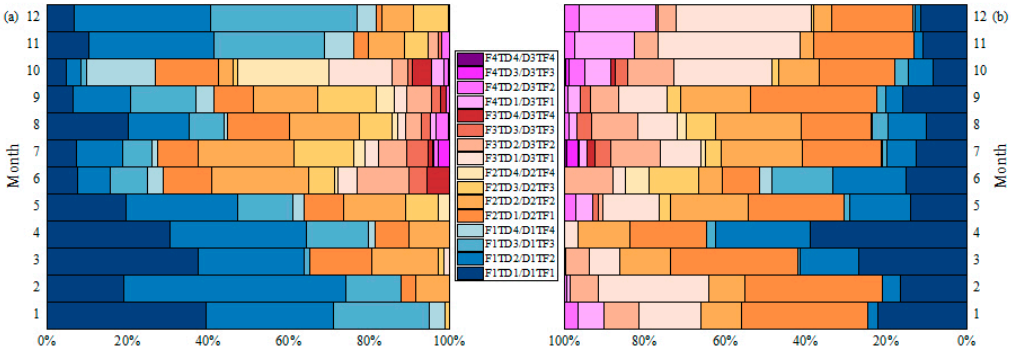

Figure 9. The percentage of (**a**) FTD events and (**b**) DTF events by month in Fujian Province from 1961 to 2021. The values 1, 2, 3, and 4 represent light, moderate, severe, and extreme floods or droughts.

3.4.2. Spatial Evolution Characteristics of DFAA Events

The frequency of DFAA events at each station from 1961 to 2021 was calculated, and the spatial pattern of frequency was obtained by IDW interpolation (Figure 10). It can be seen from Figure 10a that the annual frequency of DTF events at each station primarily falls within the range of 0.3–1.3/a, with an average value of 0.63/a. The spatial distribution exhibits a gradual increase from the northwestern to the southeastern part. Coastal stations such as Chongwu, Jinjiang, and Pingtan have the highest frequency, exceeding 1.0/a, while stations in the northwestern parts, such as Zhenghe, Guangze, and Wuyishan, have the lowest frequency, primarily ranging from 0.3~0.6/a. In Figure 10b, the annual frequency of FTD events at each station primarily falls within the range of 0.4~1.5/a with an average value of 0.80/a. The spatial pattern shows a gradually increasing trend from northwest to southeast, the frequency of the stations in the southeast coastal areas, including Chongwu, Jinjiang, Pingtan, Lianjiang, and Changle, were the largest and were all above 1.2/a, while the stations in the northwest areas had the lowest frequency, ranging from 0.4 to 0.7/a. In total, the spatial distribution of the frequency of DTF and FTD events in Fujian Province showed a similar overall trend. However, in terms of quantity, the frequency of FTD events is significantly higher than that of DTF events.

The study period was divided into three intervals: 1961–1980, 1981–2000, and 2001–2021, and the mean intensity of DTF events for these time periods is shown in Figure 11. In Figure 11a, the mean intensity of DTF events in Fujian Province from 1961 to 2021 primarily falls within the range of 2.1 to 2.5, indicating that DTF events are mainly characterized by moderate intensity. The spatial pattern reveals a gradual increase from the northwest (2.1–2.3) to the southeast (2.3–2.5). Additionally, the intensity of DTF events exhibits an upward trend during 1961~1980 and 1981–2021, The most significant change in the intensity of DTF events was found in the northern, western, and eastern regions, followed by the southern areas. In the northern and western regions, the intensity of DTF events at most stations ranged mostly between 2.1 and 2.3 from 1961 to 1980. From 1981 to 2021, it increased to 2.4 in most stations, and it increased to 2.5 in some specific stations, such as the Changting station in the western region, and the Yongan and Pucheng stations in the northern region. Among them, the most significant increase was observed in the Shaowu station in the northern region, increasing from 1.8 to 2.7. In the eastern and southern regions, the intensity of DTF events increased from 2.3 to 2.4 between 1961 and 1980 and further increased to a range of 2.4 to 2.6 between 1981 and 2021. The most significant increase was observed in the Shouning, Fuan, Zherong, and Fuding stations in the eastern region, where the intensity increased from 2.7 to 2.9.

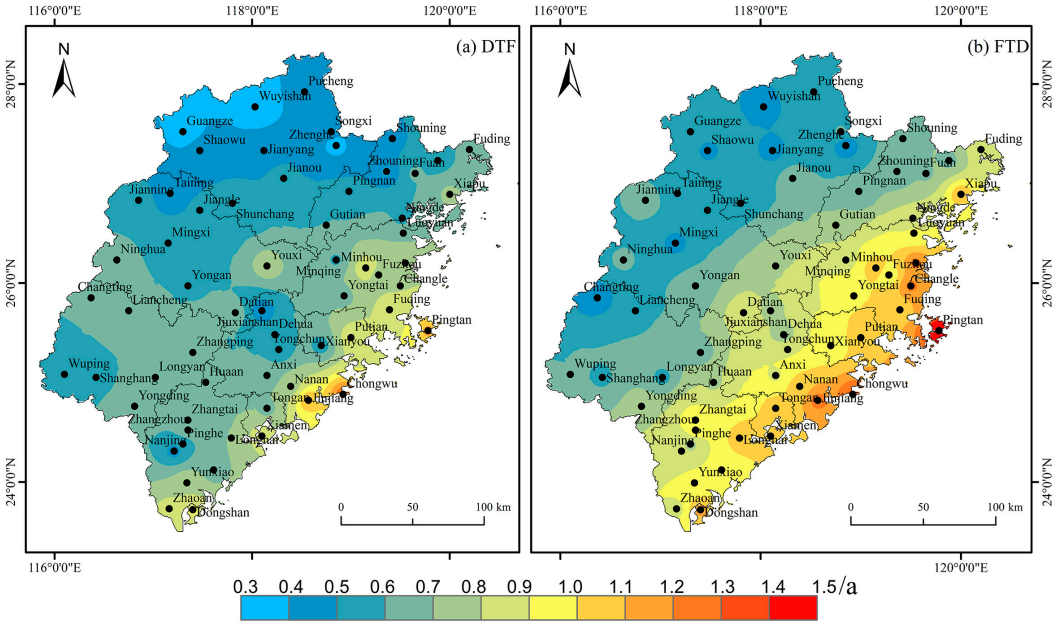

Figure 10. The spatial pattern of the frequency of DTF (**a**) and FTD events (**b**) in Fujian Province from 1961 to 2021.

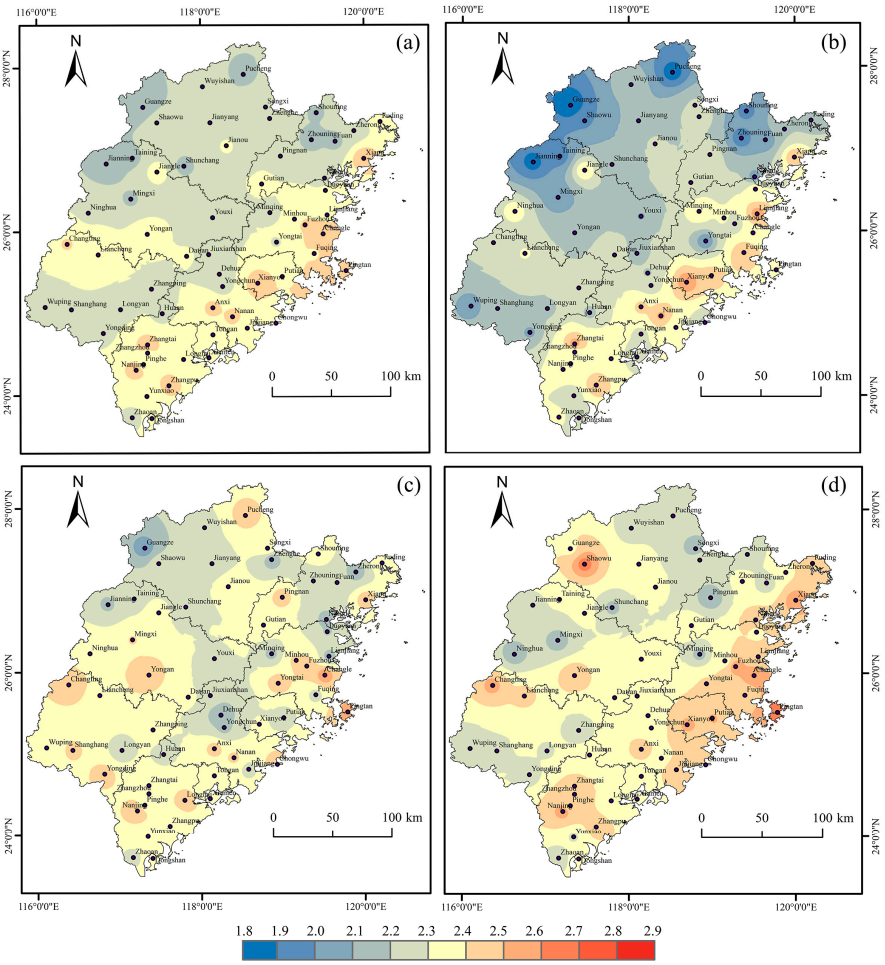

Figure 11. The changes in the intensity of DTF events in Fujian Province from 1961 to 2021. (**a**) 1961~2021/(**b**) 1961~1980/(**c**) 1981~2000/(**d**) 2001~2021 mean DTF event intensity.

As shown in Figure 12a, the average intensity of FTD events from 1961 to 2021 falls in the range of 2.2 to 2.7, with moderate-intensity events dominating. The spatial distribution revealed that the western region generally had lower intensities, around 2.3–2.4. In the rest of the region, the intensity was concentrated around 2.5–2.6, with some areas reaching an intensity of 2.7, such as Fuzhou station in the east and Shaowu station in the north. Additionally, the intensity of FTD events showed an increasing trend in the western region, particularly in Longyan City from 1961 to 2021. In Longyan City, the intensity increased from 2.0~2.3 during 1961–1980 to 2.4–2.5 during 2001–2021, except at the Zhangping station. In the northern region, there was a relatively small intensity change from 1961 to 2000, except for Jianou station where the intensity change was significant, ranging from 1.9 to 2.6. However, the change characteristic from 2001 to 2021 in the northern region the was opposite, with relatively small changes in Jianou Station, while significant changes in other regions increased from 2.3 to 2.6 to 2.4 to 2.8. In the eastern region, the intensity change was minimal, from 1961 to 2000, with the intensity primarily in the range of 2.4–2.7. However, the intensity changes in the eastern region from 2001 to 2021 were substantial, and Fuding, Zherong, and Pingtan stations experienced an increase to a maximum value of 2.9. In the southern region, the intensity has been more stable over the past 60 years, which could be attributed to the initially higher intensity (2.4 to 2.6) of FTD events, during 1961–1980.

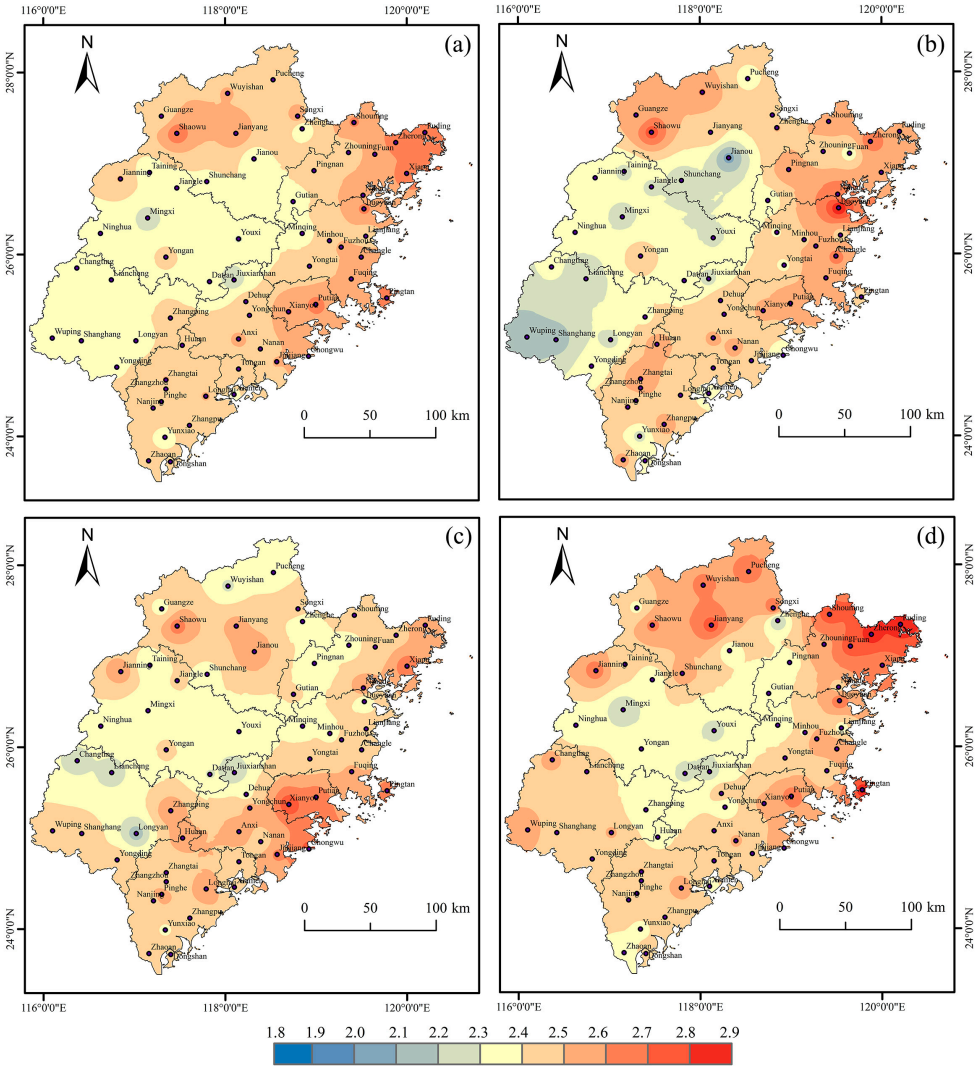

Figure 12. The changes in the intensity of FTD events in Fujian Province from 1961 to 2021. (**a**) 1961~2021/(**b**) 1961~1980/(**c**) 1981~2000/(**d**) 2001~2021 mean DTF event intensity.

4. Discussion

The number of studies to explore the spatial-temporal variations of DFAA events has increased over the past 7 years. However, the effectiveness of the identification index has not been validated and thoroughly discussed in the studies. Most studies usually adopted an index to identify DFAA events. To the best of our understanding, the optimization of different DFFA indexes has only been conducted by Liang et al. [30]. Liang et al. [30] discussed the applicability of DFAA identification indexes including the SPI, SPEI, and SWAP in identifying short-term drought-flood abrupt alternation events in the Pearl River Basin. The results by Liang et al. [30] are different from ours, and they found that the SWAP can be used as the optimal identification index of short-term DFAA events. This could be attributed to the different geographical environments in the research area.

Previous studies have shown that DFAA events predominantly took place in the central and southeastern of China [31,51]. Particularly, Fujian Province, as a representative region of southeastern China, exhibited a pattern of increasing droughts and floods, as observed by Yang et al. [52] and Wu et al. [53]. The results of this study show that FTD events exhibited an increasing trend and DTF events exhibited a slightly decreasing trend in Fujian Province during the period 1961–2021, in which the frequency of FTD events was significantly higher than the frequency of DTF events in general. The study reveals a consistent upward trend in the frequency and intensity of DFAA in Fujian Province, which aligns with similar findings in studies conducted in the Yangtze River Basin [26], the Han River Basin [23], and the Haihe River Basin [54].

DFAA events are triggered by a variety of factors, including meteorological factors [55,56] and atmospheric circulation [57]. Among them, the change in meteorological factors leads to the anomaly precipitation and temperatures then induces DFAA events. The changes in precipitation patterns in the context of global warming play a significant role [58], particularly the increase in the intensity and frequency of heavy rainfall events, leading to a higher occurrence of floods. Global warming also results in increased evaporation rates [44], which may extend the duration of drought events [59]. Additionally, drought events can be exacerbated by the overlap of droughts with high temperatures [60]. Previous studies [52,53,61] indicate an increasing trend in both droughts and floods in recent years within Fujian Province. Therefore, the frequency of DFAA events increased from 1961 to 2021 due to the frequent occurrence of droughts and floods. According to the IPCC (2021), global warming and rising temperatures, coupled with prolonged droughts and heavy precipitation, are expected to result in more frequent and severe DFAA events. These events typically have detrimental impacts on ecosystems, leading to consequences such as reduced crop yields [62] and increased water pollution [63].

Moreover, it is important to note that atmospheric circulation, such as El Niño-Southern Oscillation (ENSO), is linked to the incidence of DFAA events. Hu et al. [64] illustrated the amplified impact of ENSO on the climate under global warming and found that during ENSO warm phases, regions like Latin America and China's Yangtze River Basin are prone to floods. Additionally, the coupling of atmospheric circulation patterns and the anomalous transportation of warm, humid air leads to rapid transitions between short-term drought and flood occurrences [65].

5. Conclusions

Taking Fujian Province as a case study, this study investigated the robustness of the SPI, SPEI, and SWAP in identifying DFAA events under varying days of antecedent precipitation in the southeastern part of China and explored the spatial-temporal evolution characteristics of DFAA events in Fujian province. The main conclusions are as follows:

(1) When considering a 12-day antecedent precipitation period, the effectiveness indicated by the CI and CV and the generalization ability indicated by the weight proportion in the DFAA identification results were superior to other day values. Additionally, the weight proportion of the SPI significantly outperformed the SWAP and SPEI. SPI-12d is an effective index for meteorological DFAA event monitoring in Southeast China.

(2) There was an increasing trend in DFAA events at a rate of 1.8/10a between 1961 and 2021. DTF events showed a decreasing trend at a rate of −1.0 event/10a, while FTD events displayed an increasing trend at a rate of 2.0 event/10a. The frequencies of DTF and FTD events demonstrated a gradual increase from the northwest to the southeast.

(3) Both the DTF and FTD events were dominated by moderate events, with 62.18% and 64.57% of occurrences, respectively. DTF events were characterized by moderate drought to flood, particularly in February, July, and August. FTD events were characterized by light/moderate flood-to-drought events, with a higher occurrence of moderate flood-to-drought events observed from June to October. Notably, abrupt shifts from extreme flood to extreme drought were concentrated from October to December.

(4) Over the past 60 years, there has been a more significant increase in the intensity of DTF events in the northern and western regions of Fujian province. The intensity of FTD events showed a significant increase in the western region from 1960 to 2000, while the intensity showed a significant increase for all regions with the exception of the central region during 2001–2021.

The findings of this study provide insights into the spatial-temporal evolution characteristics of DFAA events in Fujian Province and highlight the importance of precautionary measures against DFAA events in Southeast China. Additionally, the optimization index SPI-12d can be used for the identification of DFAA events in Southeast China and other similar regions.

Author Contributions: Conceptualization, B.Z. and Y.C.; Methodology, B.Z. and Y.C.; Software, Y.C.; Formal analysis, Y.C., X.C. and M.L.; Investigation, M.L.; Resources, Y.C., X.C. and L.G.; Data curation, B.Z., L.G. and M.L.; Writing—original draft, B.Z.; Writing—review & editing, B.Z., Y.C. and L.G.; Visualization, L.G.; Project administration, X.C. and L.G.; Funding acquisition, Y.C. and X.C. All authors have read and agreed to the published version of the manuscript.

Funding: This work was supported by the National Natural Science Foundations of China (U22A20554) and the Scientific Project from Fujian Provincial Department of Science and Technology (2022Y0007).

Data Availability Statement: Data are contained within the article.

Conflicts of Interest: The authors declare no conflict of interest.

References

1. Wu, X.; Zhang, R.; Bento, V.A.; Leng, S.; Qi, J.; Zeng, J.; Wang, Q. The effect of drought on vegetation gross primary productivity under different vegetation types across China from 2001 to 2020. *Remote Sens.* **2022**, *14*, 4658. [CrossRef]
2. Wang, Q.; Qi, J.; Wu, H.; Zeng, Y.; Shui, W.; Zeng, J.; Zhang, X. Freeze-Thaw cycle representation alters response of watershed hydrology to future climate change. *Catena* **2020**, *195*, 104767. [CrossRef]
3. Sun, B.; Zhang, L.; Chen, S.; Outten, S. Editorial: Extreme climate events: Variability, mechanisms, and numerical simulations. *Front. Earth Sci.* **2023**, *11*, 1159605. [CrossRef]
4. Leng, S.; Huete, A.; Cleverly, J.; Gao, S.; Yu, Q.; Meng, X.; Qi, J.; Zhang, R.; Wang, Q. Assessing the impact of extreme droughts on dryland vegetation by multi-satellite solar-induced chlorophyll fluorescence. *Remote Sens.* **2022**, *14*, 1581. [CrossRef]
5. Leng, S.; Huete, A.; Cleverly, J.; Yu, Q.; Zhang, R.; Wang, Q. Spatiotemporal variations of dryland vegetation phenology revealed by satellite-observed fluorescence and greenness across the North Australian Tropical Transect. *Remote Sens.* **2022**, *14*, 2985. [CrossRef]
6. Zeng, J.; Zhang, R.; Qu, Y.; Bento, V.A.; Zhou, T.; Lin, Y.; Wu, X.; Qi, J.; Shui, W.; Wang, Q. Improving the drought monitoring capability of VHI at the global scale via ensemble indices for various vegetation types from 2001 to 2018. *Weather. Clim. Extrem.* **2022**, *35*, 100412. [CrossRef]
7. Chen, H.; Wang, S. Accelerated Transition Between Dry and Wet Periods in a Warming Climate. *Geophys. Res. Lett.* **2022**, *49*, e2022GL099766. [CrossRef]
8. Ford, T.W.; Chen, L.; Schoof, J.T. Variability and Transitions in Precipitation Extremes in the Midwest United States. *J. Hydrometeorol.* **2020**, *22*, 533–545. [CrossRef]
9. Ren, J.; Wang, W.; Wei, J.; Li, H.; Li, X.; Liu, G.; Chen, Y.; Ye, S. Evolution and prediction of drought-flood abrupt alternation events in Huang-Huai-Hai River Basin, China. *Sci. Total Environ.* **2023**, *869*, 161707. [CrossRef] [PubMed]
10. Wu, Z.; Li, J.; He, J.; Jiang, Z. Large-scale atmospheric singularities and summer long-cycle droughts-floods abrupt alternation in the middle and lower reaches of the Yangtze River. *Chin. Sci. Bull.* **2006**, *51*, 2027–2034. [CrossRef]
11. Zhang, S.; Zhang, J.; Min, J.; Zhang, Z.; Zhuang, J.; Lin, J. Drought-flood abrupt alternation based on runoff in the Huaihe River Basin during rainy season. *J. Lake Sci.* **2012**, *24*, 679–686.

12. Shan, L.-j.; Li-ping, Z.; Xin-chi, C.; Wei, Y. Spatio-temporal evolution characteristics of drought- flood abrupt alternation in the middle and lower reaches of the yangtze river basin. *Ecol. Inform.* **2015**, *24*, 2100–2107.
13. Shan, L.-j.; Zhang, L.; Xiong, Z.; Chen, X.; Chen, S.; Yang, W.J.M.; Physics, A. Spatio-temporal evolution characteristics and prediction of dry–wet abrupt alternation during the summer monsoon in the middle and lower reaches of the Yangtze River Basin. *Meteorol. Atmospheric Phys.* **2018**, *130*, 427–440. [CrossRef]
14. Yang, X.; Yunchuan, Y.; Simin, D.; Liping, L.; Chongxun, M.; Disasters, Y. The spatio-temporal evolution characteristics of monthly drought-flood abrupt alternation in Guangxi. *J. Nat. Disasters* **2019**, *28*, 192–203.
15. Sun, H.; Lihui, W.; Ping, T.; Pu, X.; Yong, J.; Zhiming, Y.; Qingshui, Z. Identification and Situation Analysis of Historical Drought-Flood Abrupt Alternation in Jiulong River Basin in Fujian. *Pearl. River.* **2023**, *44*, 78–86. [CrossRef]
16. Wang, R.; Li, X.; Zhang, Q.; Cheng, J.; Li, J.; Zhang, D.; Liu, Y. Projection of drought-flood abrupt alternation in a humid subtropical region under changing climate. *J. Hydrol.* **2023**, *324*, 129875. [CrossRef]
17. Wang, J.; Rong, G.; Li, K.; Zhang, J. Analysis of Characteristics of Dry–Wet Events Abrupt Alternation in Northern Shaanxi, China. *Water* **2021**, *13*, 2384. [CrossRef]
18. Bai, X.; Zhao, C.; Tang, Y.; Zhang, Z.; Yang, B.; Wang, Z. Identification, physical mechanisms and impacts of drought–flood abrupt alternation: A review. *Front. Earth Sci.* **2023**, *11*, 1203603. [CrossRef]
19. Zhang, R.; Bento, V.A.; Qi, J.; Xu, F.; Wu, J.; Qiu, J.; Li, J.; Shui, W.; Wang, Q. The first high spatial resolution multi-scale daily SPI and SPEI raster dataset for drought monitoring and evaluating over China from 1979 to 2018. *Big Earth Data* **2023**, *7*, 1–26. [CrossRef]
20. Wan, L.; Bento, V.A.; Qu, Y.; Qiu, J.; Song, H.; Zhang, R.; Wu, X.; Xu, F.; Lu, J.; Wang, Q. Drought characteristics and dominant factors across China: Insights from high-resolution daily SPEI dataset between 1979 and 2018. *Sci. Total Environ.* **2023**, *901*, 166362. [CrossRef] [PubMed]
21. Wang, Q.; Zeng, J.; Qi, J.; Zhang, X.; Zeng, Y.; Shui, W.; Xu, Z.; Zhang, R.; Wu, X.; Cong, J. A multi-scale daily SPEI dataset for drought characterization at observation stations over mainland China from 1961 to 2018. *Earth Syst. Sci. Data* **2021**, *13*, 331–341. [CrossRef]
22. Xu, F.; Qu, Y.; Bento, V.A.; Song, H.; Qiu, J.; Qi, J.; Wan, L.; Zhang, R.; Miao, L.; Zhang, X.; et al. Understanding Climate Change Impacts on Drought in China over the 21st century: A Multi-Model Assessment from CMIP6. *NPJ Clim. Atmos. Sci.* **2024**, *7*, 32. [CrossRef]
23. Zhao, Y.; Weng, Z.; Chen, H.; Yang, J. Analysis of the Evolution of Drought, Flood, and Drought-Flood Abrupt Alternation Events under Climate Change Using the Daily SWAP Index. *Water* **2020**, *12*, 1969. [CrossRef]
24. Xu, Y.; Ren, C.Y.; Ma, X.D.; Zhao, D.N.; Chen, W. Change of Drought at Multiple Temporal Scales Based on SPI/SPEI in Northeast China. *Arid Zone Res.* **2017**, *34*, 1250–1262. [CrossRef]
25. Pei, Z.; Fang, S.; Wang, L.; Yang, W. Comparative Analysis of Drought Indicated by the SPI and SPEI at Various Timescales in Inner Mongolia, China. *Water* **2020**, *12*, 1925. [CrossRef]
26. Yang, J.; Chen, H.; Hou, Y.; Zhao, Y.; Chen, Q.; Xu, C.; Chen, J. A method to identify the drought-flood transition based on the meteorological drought index. *Acta Geogr. Sin.* **2019**, *74*, 2358–2370. [CrossRef]
27. Zhou, W.; Liu, D.; Zhang, J.; Jiang, S.; Xing, S.; Wang, J.; Cheng, Y.; Chen, N. Identification and frequency analysis of drought—Flood abrupt alternation events using a daily-scale standardized weighted average of the precipitation index. *Front. Environ. Sci.* **2023**, *11*, 1142259. [CrossRef]
28. Dibs, H.; Ali, A.H.; Al-Ansari, N.; Abed, S.A. Fusion Landsat-8 Thermal TIRS and OLI Datasets for Superior Monitoring and Change Detection using Remote Sensing. *Emerg. Sci. J.* **2023**, *7*, 428–444. [CrossRef]
29. Dibs, H.; Al-Ansari, N.; Ali, A.H. Multi-Fusion Algorithms for Detecting Land Surface Pattern Changes Using Multi-High Spatial Resolution Images and Remote Sensing Analysis. *Emerg. Sci. J.* **2023**, *7*, 1215–1231. [CrossRef]
30. Liang, M.; Bingjun, L.; Dan, L. Optimization of identification index for drought-flood abrupt alternation events in the Pearl River Basin. *J. Nat. Disasters* **2022**, *31*, 57.
31. Bi, W.; Li, M.; Weng, B.; Yan, D.; Dong, Z.; Feng, J.; Wang, H. Drought-flood abrupt alteration events over China. *Sci. Total Environ.* **2023**, *875*, 162529. [CrossRef]
32. Xie, Y.; Liu, Z.; Lin, K. Dry-Wet Transition Events in China: Identification, Temporal Dynamics, and Spatial Patterns. *J. Yangtze River Sci. Res. Inst.* **2021**, *38*, 77–85. [CrossRef]
33. Wang, S.; Tian, H.; Ding, X. Climate Characteristics of Precipitation and Phenomenon of Drought-flood Abrupt Alternation during Main Flood Season in Huaihe River Basin. *Chin. J. Agrometeorol.* **2009**, *30*, 31–34.
34. Liu, B.; Jianyu, F.; Manlin, L.; Yadong, J. Spatio-temporal evolution trend analysis of drought and flood disasters in the Pearl River Basin. *China Flood Drought Manag.* **2023**, *33*, 12–19+45. [CrossRef]
35. Jiang, S.; Cui, H.; Ren, L.; Yan, D.; Yang, X.; Yuan, S.; Liu, Y.; Wang, M.; Xu, C.-Y. Will China's Yellow River basin suffer more serious combined dry and wet abrupt alternation in the future? *J. Hydrol.* **2023**, *624*, 129871. [CrossRef]
36. Arianti, I.; Rafani, M.; Fitriani, N.A.; Nizar, J. Spatial Modeling of Flood-Vulnerability as Basic Data for Flood Mitigation. *Civ. Eng. J.* **2023**, *9*, 787–798. [CrossRef]
37. Mckee, T.B.; Doesken, N.J.; Kleist, J.R. The relationship of drought frequency and duration to time scales. In Proceedings of the 8th Conference on Applied Climatology, Anaheim, CA, USA, 17–22 January 1993.

38. Vicente-Serrano, S.M.; Beguería, S.; López-Moreno, J.I. A Multiscalar Drought Index Sensitive to Global Warming: The Standardized Precipitation Evapotranspiration Index. *J. Clim.* **2009**, *23*, 1696–1718. [CrossRef]
39. Lu, E. Determining the start, duration, and strength of flood and drought with daily precipitation: Rationale. *Geophys. Res. Lett.* **2009**, *36*. [CrossRef]
40. Lu, E.; Lu, E.; Cai, W.; Jiang, Z.; Zhang, Q.; Zhang, C.; Higgins, R.W.; Halpert, M.S. The day-to-day monitoring of the 2011 severe drought in China. *Clim. Dyn.* **2014**, *43*, 1–9. [CrossRef]
41. Gu, L.; Chen, J.; Yin, J.; Xu, C.-Y.; Chen, H. Drought hazard transferability from meteorological to hydrological propagation. *J. Hydrol.* **2020**, *585*, 124761. [CrossRef]
42. Achite, M.; Krakauer, N.Y.; Wałęga, A.; Caloiero, T. Spatial and Temporal Analysis of Dry and Wet Spells in the Wadi Cheliff Basin, Algeria. *Atmosphere* **2021**, *12*, 798. [CrossRef]
43. Rezvani, R.; RahimiMovaghar, M.; Na, W.; Reza Najafi, M. Accelerated Lagged Compound Floods and Droughts in Northwest North America under 1.5–4 °C Global Warming Levels. *J. Hydrol.* **2023**, *624*, 129906. [CrossRef]
44. Chen, H.; Wang, S.; Zhu, J.; Zhang, B. Projected Changes in Abrupt Shifts Between Dry and Wet Extremes Over China Through an Ensemble of Regional Climate Model Simulations. *J. Geophys. Res. Atmos.* **2020**, *125*, e2020JD033894. [CrossRef]
45. Li, X.G.; Han, G.X.; Zhu, L.Q.; Chen, C.N. Effects of drying-wetting cycle caused by rainfall on soil respiration: Progress and prospect. *Chin. J. Ecol.* **2019**, *38*, 567–575.
46. Du, J.; Fang, J.; Xu, W.; Shi, P.; Assessment, R. Analysis of dry/wet conditions using the standardized precipitation index and its potential usefulness for drought/flood monitoring in Hunan Province, China. *Stoch. Environ. Res. Risk Assess.* **2013**, *27*, 377–387. [CrossRef]
47. Gao, G. Research on the method of determining indicator weights and converting scores in multi-indicator comprehensive evaluation. *J. China Economist.* **2003**, *3*, 265–266.
48. Yan, B.; Qian, J.; Guo, C. Comprehensive Indicator Weight Determination and Application Based on Dynamic Weight. *J. Shenyang Agric. Univ.* **2014**, *45*, 58–61.
49. Wen, K. *China Meteorological Disaster Dictionary*; China Meteorological Press: Beijing, China, 2007.
50. Fujian-Meteorological-Bureau. Weather Chian. Available online: http://fj.weather.com.cn/zxfw/qhgb/index.shtml (accessed on 1 January 2001).
51. Qiao, Y.; Xu, W.; Wu, D.; Meng, C.; Qin, L.; Li, Z.; Zhan, X. Changes in the spatiotemporal patterns of dry/wet abrupt alternation frequency, duration, and severity in Mainland China, 1980–2019. *Sci. Total Environ.* **2022**, *838*, 156521. [CrossRef]
52. Yang, X.; Rongyan, Z.; Hang, P.A.N.; Shiyan, G.A.O.; Chen, Y.U.; Ruijuan, B.A.O. Spatio-Temporal Distribution Analysis of Multi-Dimensional Meteorological Drought Characteristics in Fujian Province. *Meteorol. Mon.* **2022**, *48*, 1565–1576. [CrossRef]
53. Wu, B.; Li, L. Study on the effect of precipitation tendency change on drought/flood in fujian province. *J. Trop. Meteorol.* **2009**, *25*, 103–109.
54. Ang, Y.; Chen, Y.; Chen, S.; Xiong, M. Spatial and temporal variation characteristics of the drought-flood abrupt alternations over Haihe River Basin. *Hydro-Sci. Eng.* **2021**, 1–12. [CrossRef]
55. Shi, W.; Zhang, K.; Xie, Y.; Chao, L.; Tola, T.L.; Xue, X. Monitoring the Variation of Drought-Flood Abrupt Alternation and Its Response to Atmospheric Circulation at Multi-time Scales. In *Proceedings of PIANC Smart Rivers 2022*; Li, Y., Hu, Y., Rigo, P., Lefler, F.E., Zhao, G., Eds.; Springer: Singapore, 2023; pp. 1139–1151.
56. Sun, J.; He, J.; Ren, J.; Zhong, S.; Wang, L. Analysis of the relationship between the precipitation and the SST based on the TRMM data during the Asia monsoon season. In *Earth Observing Systems XI*; SPIE: Bellingham, WA, USA, 2006; pp. 295–306.
57. Zhang, Y.; Zhai, L.; Lin, P.; Cheng, L.; Wei, X. Variation characteristics and driving factors of drought and flood and their abrupt alternations in a typical basin in the middle reaches of Yangtze River. *Eng. J. Wuhan Univ.* **2021**, *54*, 887–897.
58. Zhang, R.; Qi, J.; Leng, S.; Wang, Q. Long-Term Vegetation Phenology Changes and Responses to Preseason Temperature and Precipitation in Northern China. *Remote Sens.* **2022**, *14*, 1396. [CrossRef]
59. Zarch, M.A.A.; Sivakumar, B.; Sharma, A. Droughts in a warming climate: A global assessment of Standardized precipitation index (SPI) and Reconnaissance drought index (RDI). *J. Hydrol.* **2015**, *526*, 183–195. [CrossRef]
60. Wright, B.; Stanford, B.; Weiss, J.; Debroux, J.; Routt, J.; Khan, S. Climate Change how does Weather Affect Surface Water Quality. *Opflow* **2013**, *39*, 10–15. [CrossRef]
61. Chou, J.; Xian, T.; Dong, W.; Xu, Y. Regional Temporal and Spatial Trends in Drought and Flood Disasters in China and Assessment of Economic Losses in Recent Years. *Sustainability* **2019**, *11*, 55. [CrossRef]
62. Huang, J.; Hu, T.; Yasir, M.; Gao, Y.; Chen, C.; Zhu, R.; Wang, X.; Yuan, H.; Yang, J. Root growth dynamics and yield responses of rice (*Oryza sativa* L.) under drought—Flood abrupt alternating conditions. *Environ. Exp. Bot.* **2019**, *157*, 11–25. [CrossRef]
63. Bi, W.; Weng, B.; Yan, D.; Wang, M.; Wang, H.; Jing, L.; Yan, S. Soil phosphorus loss increases under drought-flood abrupt alternation in summer maize planting area. *Agric. Water Manag.* **2022**, *262*, 107426. [CrossRef]

64. Hu, K.; Huang, G.; Huang, P.; Kosaka, Y.; Xie, S.-P. Intensification of El Niño-induced atmospheric anomalies under greenhouse warming. *Nat. Geosci.* **2021**, *14*, 377–382. [CrossRef]
65. Xue, Y.; Xue, X. Research advances in simultaneous frequency of extreme precipitation and drought. *J. Mar. Meteorol.* **2022**, *42*, 61–73.